Soft Matter

ROYAL SOCIETY OF CHEMISTRY

ARTICLE TYPE

Cite this: DOI: 10.1039/xxxxxxxxxx

A simple strategy to improve the interfacial activity of true Janus gold nanoparticles: a shorter hydrophilic capping ligand†

Miguel Angel Fernandez-Rodriguez,[a] Limei Chen,[b] Christopher P. Deming,[b] Miguel Angel Rodriguez-Valverde,[a] Shaowei Chen,[b] Miguel Angel Cabrerizo-Vilchez,[a] and Roque Hidalgo-Alvarez*[a]

Received Date
Accepted Date

DOI: 10.1039/xxxxxxxxxx

www.rsc.org/journalname

Janus gold nanoparticles (JPs) of $\sim$ 4 nm-diameter half functionalized with 1-hexanethiol as hydrophobic capping ligand exhibit significantly higher interfacial activity, reproducibility and rheological response when the other half is functionalized with 1,2-mercaptopropanediol (JPs-MPD) than with 2-(2-mercaptoethoxy)ethanol (JPs-MEE), both acting as the hydrophilic capping ligand. The interfacial pressure measured by pendant drop tensiometry reaches 50 mN/m and 35 mN/m for the JPs-MPD at the water/air and water/decane interface, respectively. At the same area per particle, the JPs-MEE reveal significantly lower interfacial pressure: 15 mN/m and 5 mN/m at the water/air and water/decane interface, respectively. Interfacial dilatational rheology measurements also show an elastic shell behaviour at higher compression states for JPs-MPD while the JPs-MEE present near-zero elasticity. The enhanced interfacial activity of JPs-MPD is explained in terms of chemical and hydration differences between the MPD and MEE ligands, where MPD has a shorter hydrocarbon chain and twice more hydroxyl terminal groups than MEE.

Pickering emulsions can be thermodynamically stabilized by amphiphilic Janus nanoparticles (JPs) with a wettability anisotropy[1–3].It is known that JPs show three times more adsorption energy than homogeneous nanoparticles[2,4]. Strong efforts have been made to synthesize and simulate JPs with different morphologies and surface chemistry to control the way in which these particles self-assemble at fluid interfaces[5–9].

Gold nanoparticles randmonly functionalized with 1-undecanethiol and N,N,N-trimethyl (11-mercaptoundecyl) ammonium chloride are reported to become Janus-like when the capping ligands rearrange at the water/air interface[10]. Nevertheless, recently Reguera et al.[11] demonstrated by neutron reflectivity that such rearrangement does not happen with gold nanoparticles functionalized with 1-octanethiol and 6-mercapto-1-hexanol at the water/air interface. A way to obtain gold JPs with true separate domains is to selectively functionalize each hemisphere of the core with the desired capping ligands immobilizing the nanoparticles in a Langmuir balance[12,13].

It is fundamental to select the appropiate capping ligands that will confer the Janus character to the nanoparticles because of the significant dependence between these capping ligands and the interfacial activity of the final JPs. We propose a simple strategy to enhance the interfacial activity, rheological response and reproducibility through colloidal stability of true gold Janus nanoparticles. We synthesized Janus gold nanoparticles half capped by 1-hexanethiol and the other half by 2-(2-mercapto-ethoxy)ethanol (JPs-MEE) or 1,2-mercaptopropanediol (JPs-MPD) in surfactant-free conditions as described in previous works (see Fig. 1)[12–14]. The sizes obtained by high resolution TEM measurements (see Fig. S1†) are $3.5 \pm 0.9\,nm$ and $3.7 \pm 1.9\,nm$ for the JPs-MEE and JPs-MPD, respectively. The electrophoretic mobility of both JPs was measured with a ZetaSizer Nano (Malvern) in a $10^{-2}\,M$ sodium citrate MilliQ water solution to stabilize the electrical double layer obtaining $\mu_{e,JPs-MEE} = (-2.2 \pm 1.5) \cdot 10^{-8}\,m^2/(V \cdot s)$ and $\mu_{e,JPs-MPD} = (-2.9 \pm 0.4) \cdot 10^{-8}\,m^2/(V \cdot s)$. From previous works, the JPs-MEE showed an average macroscopic contact angle of $(56.1 \pm 1.8)^\circ$ and $(49.0 \pm 1.3)^\circ$ in each hemisphere, whereas the JPs-MPD showed $(63.3 \pm 2.7)^\circ$ and $(53.4 \pm 2.9)^\circ$ in their respective hydrophobic and hydrophilic hemispheres[12,13]. The contact angles are slightly lower for the JPs-MEE likely due to the fabrication process: for MEE adsorption, the close-packed monolayer of 1-hexanethiol covered gold nanoparticles was immersed in a water solution containing MEE[13] and this might produce greater

[a] Biocolloid and Fluid Physics Group, Applied Physics Department, Faculty of Sciences, University of Granada, Granada, Spain; E-mail: rhidalgo@ugr.es
[b] Department of Chemistry and Biochemistry, University of California, 1156 High Street, Santa Cruz, CA 95064, USA.

† Electronic Supplementary Information (ESI) available: HRTEM micrographies and pendant drops pictures. See DOI: 10.1039/b000000x/

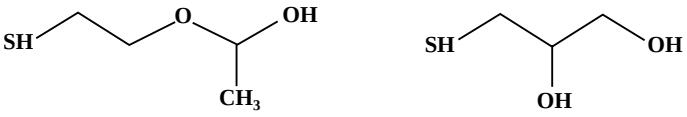

Fig. 1 MEE (left) and MPD (right) capping ligands. The *SH* group is the anchor group at the gold nanoparticle surface.

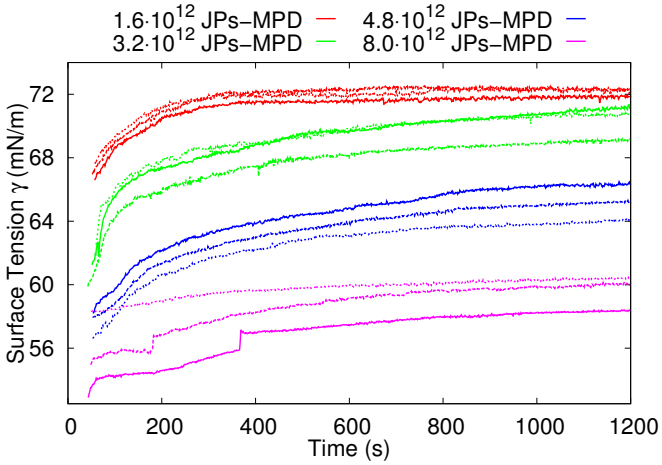

Fig. 2 Surface tension evolution over the time after the deposition of different number of JPs-MPD in THF on the surface of an initial $5\,\mu L$ MilliQ water pendant drop and growth up to $45\,\mu L$. Same color curves correspond to different experiments with the same number of deposited JPs-MPD. After the solvent evaporation, the surface tension remained stable.

hydrophilic capping ligand exchange and thus lower contact angle than for the JPs-MPD in which the functionalization with MPD was performed directly in the Langmuir balance, exchanging the MPD ligands from the water subphase[12]. The contact angle values in the hydrophilic hemispheres are similar within errors, which reflects that the differences between MPD and MEA are not reflected macroscopically in the contact angle and the wettability contrast (i.e. contact angle differences between hemispheres) is similar in both JPs-MEE and JPs-MPD within errors. The pendant drop tensiometry was conducted as follows: different amounts of Janus nanoparticles (JPs-MEE and JPs-MPD) dispersed in tetrahydrofuran (THF, HPLC grade) were deposited on a water pendant drop with a handheld microsyringe and a micropositioner. The surface tension was obtained by axisymmetric drop shape analysis upon THF evaporation, while the pendant drop volume was kept constant. The results in Fig. 2 show a decrease in the final surface tension after evaporation of THF which is higher as the concentration of JPS-MPD is increased (refer to previous work for the JPs-MEE similar characterization[15]). The experiments are highly reproducible as can be seen in the different runs for a fixed concentration of JPs (different curves with same color in Fig. 2).

After the THF evaporation, growing and shrinking experiments were performed at $0.08\,\mu L/s$ for each JP concentration. Next, the pendant drop was immersed in decane and the growing and shrinking experiments were performed again. We plot the interfacial pressure ($\Pi = \gamma_0 - \gamma$, where γ_0 is $72.5 mN/m$ for the water/air (W/A) and $52.3 mN/m$ for the water/decane (W/O) interfaces and γ is the measured interfacial tension) against the drop area per particle (A_p, the area of the pendant drop divided by the number of deposited JPs). A piecewise compression isotherm can be seen in Fig. 3a and Fig. 3b for W/A and W/O interfaces, respectively. The first remarkable fact is the lower interfacial activity of JPs-MEE compared to JPs-MPD at the same A_p values. At the lowest A_p reached for JPs-MPD, Π is $50 mN/m$ and $35 mN/m$ and $15 mN/m$ and $5 mN/m$ for the JPs-MEE at the W/A and W/O interfaces, respectively. The highest Π values obtained for JPs-MEE, after further compression, are $30 mN/m$ and $20 mN/m$ at the W/A and W/O interfaces, respectively. Contrary to JPs-MEE, the compression isotherms for JPs-MPD at the W/A interface exhibit open cycles at the beginning of the experiments pointing out that the colloidal monolayer rearranges into a final state that is preserved in further compression cycles. This behaviour is attenuated at the W/O interface as the hysteresis cycles are much smaller (i.e. the upper compression and lower expansion curves are closer) which might be due to the fact that enough energy is provided to reach a more relaxed state when it is immersed in decane. Moreover, the low hysteresis of the JPs-MEE compression cycles compared to the JPs-MPD might be due to the lower interfacial activity of these particles. Since the fabrication process, hydrophobic capping ligand, wettability contrast, size and charge were similar for both JPs-MEE and JPs-MPD, the differences between interfacial activity must come from the interfacial activity of the MEE and MPD hydrophilic capping ligands. Whereas MEE has a longer hydrocarbon chain (four CH_2 and one oxygen) and one hydroxyl terminal group, the MPD has a shorter hydrocarbon chain (three CH_2) and two hydroxyl terminal groups (see Fig. 1). The lower number of hydrocarbon groups and higher number of hydroxyl groups of MPD might result in higher hydration of the hydrophilic hemisphere of the JPs (i.e. establishing hydrogen bonds between water and the hydrophilic capping ligands). These chemical differences might play a decisive role in the final interfacial activity of these JPs.

The interfacial dilatational rheology of the JPs was evaluated by ten periodic volume variations of $1\,\mu L$ for different periods. When a periodic injection/extraction of volume is performed to the pendant drop, the interface tries to re-establish the equilibrium. This counteraction is represented by a complex quantity composed by a storage part and a loss part:

$$E = E_d + i\omega\eta_d \qquad (1)$$

where E is the surface dilatational modulus that accounts for the change in surface tension produced by a small change in a surface area, E_d is the interfacial dilatational elasticity, ω is the oscillation frequency and η_d is the interfacial dilatational viscosity[16]. If the viscosity is negligible during the relaxation process after perturbation of the interface, the interface present an essentially elastic behavior. The extraordinary interfacial activity of JPs-MPD is reflected in the rheology results in Fig. 4a and 4b (see Fig. S2 and S3[†]). For both W/A and W/O interfaces, E decreases slightly and η increases for increasing periods. For the W/A interface, E_d and η_d increases clearly with the compression state of the colloidal monolayer. This trend is also observed for the W/O inter-

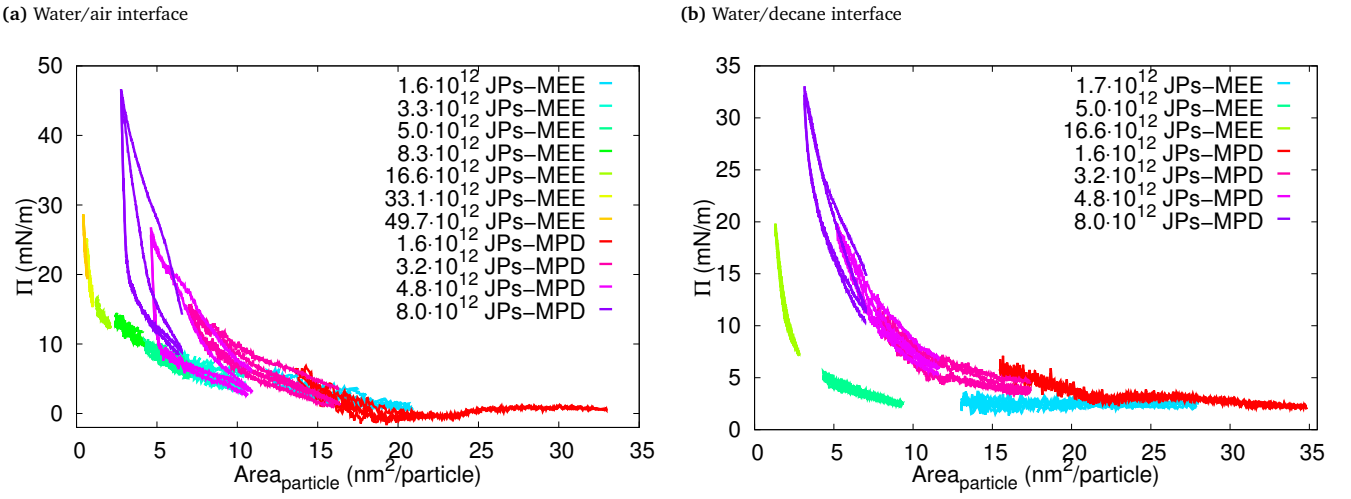

Fig. 3 Surface pressure against the area per particle for different number of JPs-MEE and JPs-MPD deposited at the **(a)** W/A and **(b)** W/O interfaces. For a more detailed characterization of the JPs-MEE, please refer to Fernandez et al.[15]

face but with lower values of both E_d and η_d. The high E_d value is a signal that the colloidal monolayer creates an elastic shell on the pendant drop at higher compression states. This elastic behaviour again suggests the ability of the JPs-MPD as emulsifiers. Further rheology experiments were performed for a fixed period of $10\,s$ comparing the response of JPs-MEE and JPs-MPD. The results in Fig. 4c and 4d point out that the JPs-MPD reach significantly higher E_d and η_d values upon compression (i.e. lower A_p) than the JPs-MEE (~ 10 times higher E_d and η_d for JPs-MPD than JPs-MEE at the W/A interface and 2 times at the W/O interface), suggesting that the elastic shell behaviour is not present for the JPs-MEE. A final consideration must be taken into account for gold nanoparticles in the range of a few nanometers (i.e. less than $10\,nm$), the adsorption energy at the interface is of the order of K_BT[17] and they are expected to easily leave the interface. Nevertheless, the stable interfacial tension over time after the THF evaporation, the closed growing/shrinking cycles and the dilatational rheology seem to point out that the JPs-MEE and JPs-MPD are irreversibly anchored at the W/A and W/O interfaces, probably due to its Janus character.

In conclusion, the JPs-MEE and JPs-MPD are similar in fabrication process, hydrophobic capping ligand, wettability contrast, size and charge, but are functionalized with different hydrophilic capping ligand. The JPs-MPD exhibit a significantly higher interfacial activity at W/A and W/O interfaces. Moreover, the dilatational rheology suggests an elastic shell-like behaviour of the pendant drop when the JPs-MPD are deposited at W/A and W/O interfaces. This elastic shell behaviour seems to be absent with the JPs-MEE. This points out the importance of the chemical structure of the capping ligands in JPs to predict the interfacial activity and therefore their ability as emulsifiers. Shorter hydrocarbon chain and more hydroxyl terminal groups in the hydrophilic capping ligands seems to be a route to obtain enhanced interfacial activity of this kind of JPs via enhanced hydration of the hydrophilic hemisphere of the JPs. To the best of our knowledge, it is the first time that such high interfacial activity is obtained with $\sim 4\,nm$-diameter gold nanoparticles in surfactant-free conditions.

Acknowledgements

This work was supported by the Spanish MINECO (projects MAT2013-44429-R and MAT2014-60615R), by "Junta de Andalucía" and FEDER (projects P10-FQM-5977 and P12-FQM-1443) and by US National Science Foundation (DMR-1409396). Authors thank to Dr. J.A. Holgado-Terriza for the software Contacto© used for surface tension measurements.

References

1 J. Hu, S. Zhou, Y. Sun, X. Fang and L. Wu, *Chem. Soc. Rev.*, 2012, **41**, 4356–4378.
2 A. Kumar, B. J. Park, F. Tu and D. Lee, *Soft Matter*, 2013, **9**, 6604–6617.
3 B. T. T. Pham, C. H. Such and B. S. Hawkett, *Polym. Chem.*, 2015, **6**, 426–435.
4 R. Aveyard, *Soft Matter*, 2012, **8**, 5233–5240.
5 A. Walther and A. H. E. Muller, *Janus Particle Synthesis, Self-Assembly and Applications*, The Royal Society of Chemistry, 2012, pp. 1–28.
6 J. Du and R. K. O'Reilly, *Chem. Soc. Rev.*, 2011, **40**, 2402–2416.
7 B. J. Park, T. Brugarolas and D. Lee, *Soft Matter*, 2011, **7**, 6413–6417.
8 H. Rezvantalab and S. Shojaei-Zadeh, *Soft Matter*, 2013, **9**, 3640–3650.
9 Z.-W. Li, Z.-Y. Lu, Z.-Y. Sun and L.-J. An, *Soft Matter*, 2012, **8**, 6693–6697.
10 Y. Song, X. Liu and S. Chen, *Functional Nanometer-Sized Clusters of Transition Metals: Synthesis, Properties and Applications*, The Royal Society of Chemistry, 2014, pp. 407–433.
11 J. Reguera, E. Ponomarev, T. Geue, F. Stellacci, F. Bresme and M. Moglianetti, *Nanoscale*, 2015, **7**, 5665–5673.

(a) Interfacial dilatational elasticity E_d

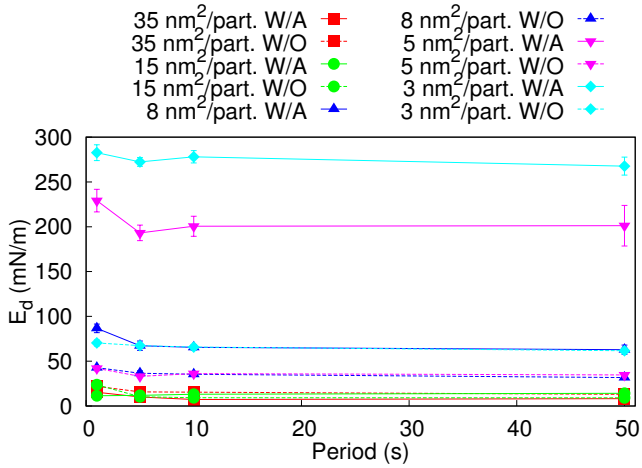

(b) Interfacial dilatational viscosity η_d

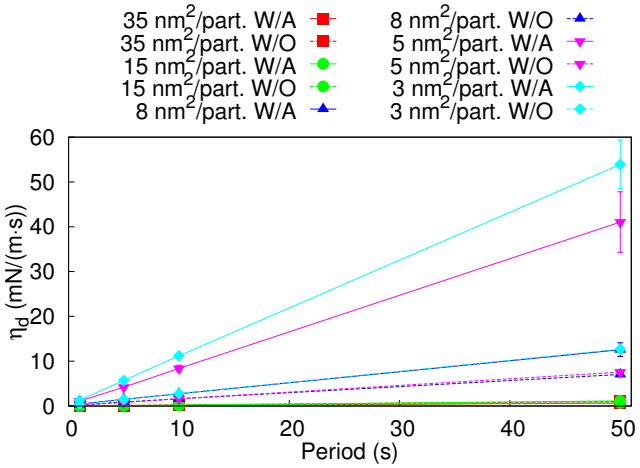

(c) Interfacial dilatational elasticity E_d for $10\,s$ period

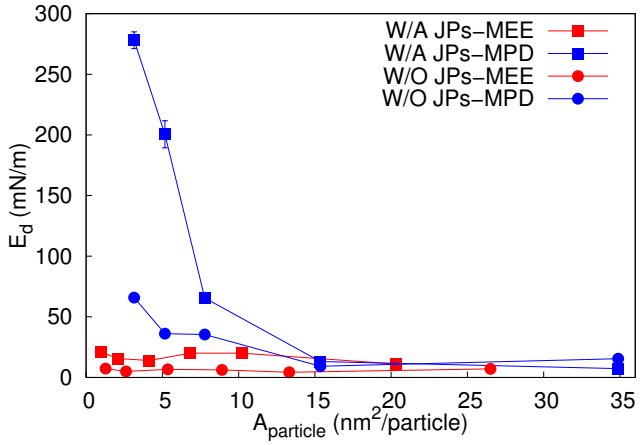

(d) Interfacial dilatational viscosity η for $10\,s$ period

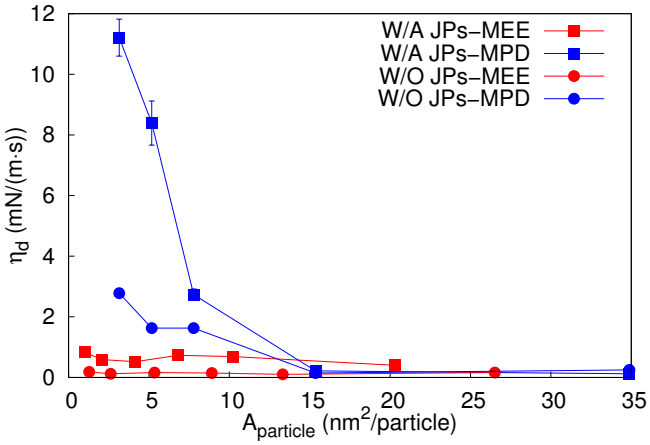

Fig. 4 (a) Interfacial dilatational elastic modulus (E_d) and **(b)** viscosity (η_d) of JPs-MPD against different periods for different A_p compression states at the W/A and W/O interfaces. **(c)** E_d and **(d)** η_d of JPs-MEE and JPs-MPD against the A_p at the W/A and W/O interfaces, for $10\,s$ period.

12 S. Pradhan, L. Xu and S. Chen, *Adv. Funct. Mater.*, 2007, **17**, 2385–2392.
13 S. Pradhan, L. Brown, J. Konopelski and S. Chen, *J. Nanopart. Res.*, 2009, **11**, 1895–1903.
14 Y. Song and S. Chen, *Chem. Asian J.*, 2014, **9**, 418–430.
15 M. A. Fernandez-Rodriguez, Y. Song, M. A. Rodriguez-Valverde, S. Chen, M. A. Cabrerizo-Vilchez and R. Hidalgo-Alvarez, *Langmuir*, 2014, **30**, 1799–1804.
16 K. C. Powell and A. Chauhan, *Langmuir*, 2014, **30**, 12287–12296.
17 S. Jiang and S. Granick, *Janus Particle Synthesis, Self-Assembly and Applications*, The Royal Society of Chemistry, 2012, pp. 244–256.